The Response of Wind-Wave Spectra to Changing Winds. Part I: Increasing Winds

YOSHIAKI TOBA

Department of Geophysics, Tohoku University, Sendai, Japan

KOZO OKADA

Japan Weather Association, Chiyoda-Ku, Tokyo, Japan

IAN S. F. JONES

Marine Studies Centre, The University of Sydney, New South Wales, Australia

(Manuscript received 22 May 1987, in final form 4 February 1988)

ABSTRACT

Continuous time series of wind profiles and wind waves under growing conditions, recorded at Shirahama Oceanographic Tower Station and discussed by Kawai, Okada and Toba, have been reanalysed for this study of the response of one-dimensional wind-wave frequency spectra to unsteady rising winds. The factor α_s in the equilibrium-range spectral form $\phi(\sigma) = \alpha_s g u_* \sigma^{-4}$ (g is gravity, σ is angular frequency and u_* is the friction velocity) shows a remarkable fluctuation. It becomes smaller for increasing wind conditions (i.e., increasing friction velocity) and larger for decreasing wind conditions within a range of (5–9) $\times 10^{-2}$. The slope of the spectra is very close to σ^{-4} generally, but it has a tendency to be slightly steeper for decreasing winds. The peak of the spectra is broader for increasing winds, and narrower for decreasing winds, when fluctuations of several-minute duration of u_* are considered. The time scale of the adjustment of the equilibrium-range spectra is on the order of ten minutes. This time scale is much faster than the time scale of growth of the total energy of the wind waves, and consequently the peak frequency shifts to higher frequencies for increasing u_*, or vice versa. This response suggests that the processes of the adjustment of the wind-wave field involve both upward and downward cascading of the wave energy. Further evidence is presented in the form of ocean wave data recorded in Bass Strait, Australia, where the waves, although much larger, show similar trends.

1. Introduction

Determining the energy spectral form is one of the central problems of modern wind-wave studies. Postulating that the breaking process of surface gravity waves imposes an upper limit to the spectral density of wave components over wave numbers substantially greater than that of the spectral peak, Phillips (1958) proposed, on dimensional grounds, a form of one-dimensional frequency spectral density $\phi(\sigma)$ of wind waves for the equilibrium range as

$$\phi(\sigma) = \beta g^2 \sigma^{-5}, \tag{1}$$

where σ is the angular frequency, g the acceleration of gravity, and the proportionality factor β was considered a dimensionless constant.

Based on empirical data from various sources and on the assumption that the wind-wave field quickly evolves toward a local equilibrium, Toba (1972) proposed, with the aid of dimensional analysis, a similarity law for wind waves, the three-second power law:

$$H^* = BT^{*3/2}, \quad B = 0.062, \tag{2}$$

where $H^* = gH/u_*^2$, $T^* = gT/u_*$, H is the significant wave height, T the significant wave period, and B an empirical constant. Toba (1973) also proposed, by assuming a self-similarity in the spectral form, which is consistent with the three-second power law (2), another form for the high-frequency side of the spectral peak:

$$\phi(\sigma) = \alpha_s g_* u_* \sigma^{-4}, \quad g_* = g\left(1 + \frac{Sk^2}{\rho_w g}\right) \tag{3}$$

with α_s as a constant, where S is the surface tension, k the wavenumber and ρ_w the density of water. Equations (2) and (3) were supported by field observation data of Kawai et al. (1977), and were used in the TOHOKU Wave Model (Joseph et al. 1981; Toba et al. 1985a,b). In recent years, the frequency dependence implied by (3) has been supported by further experimental evidence in Mitsuyasu et al. (1980), Kahma (1981), For-

Corresponding author address: Professor Yoshiaki Toba, Department of Geophysics, Tohoku University, Physical Oceanography Laboratory, Sendai 980, Japan.

ristall (1981), Donelan et al. (1985), and Battjes et al. (1987).

Kitaigorodskii (1983) derived a minus fourth frequency dependence on the assumption that the wind energy input was at low frequencies and that dissipation occurred only at high frequencies, with the energy transfer from low to high wavenumbers for the equilibrium range of frequencies. By making different assumptions, i.e., that in the balance of wave action spectral density, the spectral flux divergence by nonlinear interactions among different wave groups, input from the wind and dissipation by wave-breaking, are of the same order of magnitude and are proportional with one another, Phillips (1985) derived the spectral form (3), though he used g instead of g_*. He also pointed out the difference in observed values of α_s, which ranged between (6 and 11) $\times 10^{-2}$. Phillips (1985) assumed that, for the components whose wavenumbers are large compared with those of the spectral peak, the time scales of their internal processes are small compared with the rate of change of their energy.

The assumption of Toba (1972) for the local balance (or local equilibrium) of wind waves under the action of wind implicitly requires that the time scale of internal processes for the adjustment of the spectral form be short compared with the time scale of evolution of gross measures such as H or T. We know that under steady wind conditions, the evolution of the wave field is slow.

In the present paper, it is demonstrated that the time scale of the adjustment processes of waves to perturbation of the winds is very short, of the order of several minutes, even for frequencies up to the peak frequency of $\sigma_p = 2$ rad s^{-1} which we observed in one set of data.

The level of the spectral density in the equilibrium range follows the wind stress but lags behind it. The value of α_s varies to reflect this lag in response to the wind speed, but the slope of the spectrum of the equilibrium range keeps close to σ^{-4}. Such fluctuations of the spectra are presented in section 4.

That a local similarity for wind waves should exist is of interest. Recently, one of the authors (Toba 1987) proposed a new concept of "wind-wave breaking adjustment" as a physical interpretation of the similarity laws of wind waves. Considerable data supported this concept. This model envisages that the wind waves adjust themselves by wave breaking under the overall constraints for the coupling of the two-sided turbulent boundary layer of air and water. The local equilibrium conditions require proportionalities among characteristic velocities related to air–water interface processes. We expect that the adjustment of the wind waves to the change of wind will occur as one aspect of the adjustment of the coupled turbulent boundary layers of the air and the water, and will include strongly nonlinear processes. The present paper presents one aspect of the adjustment processes in the form of the response of wave spectra to changing winds.

2. Dataset used

The data used in this paper are from two sites. Observational data on air–sea boundary processes at the Shirahama Oceanographic Tower Station of Kyoto University were obtained in November 1969 (Toba et al. 1971). The data have already been used by Kawai et al. (1977) in support of the spectral form (3) as well as the $^3/_2$-power law (2). The data comprise two series: Series A is a five-hour record under conditions of growing winds and waves, presented every 15 minutes; series B is a 30-minute continuous record in the middle of Series A. The details of the conditions of observation may be found in Toba et al. (1971) and Kawai et al. (1977). The second sequence of data (Series C) was obtained from the Kingfish platform (38°36′S, 148°11′E) in Bass Strait, as described below.

The Kingfish B oil production platform stands in approximately 77 m of water. Wind speed and direction were sensed using a Synchrotrac wind speed and direction transmitter initially situated on a tower 37 m above mean sea level. After a correction for height, the friction velocity was calculated from this speed by Wu (1980) using the expression $u_* = (8 \times 10^{-4} + 6.5 \times 10^{-5} U_{10})^{1/2} U_{10}$. The water height was sensed with a

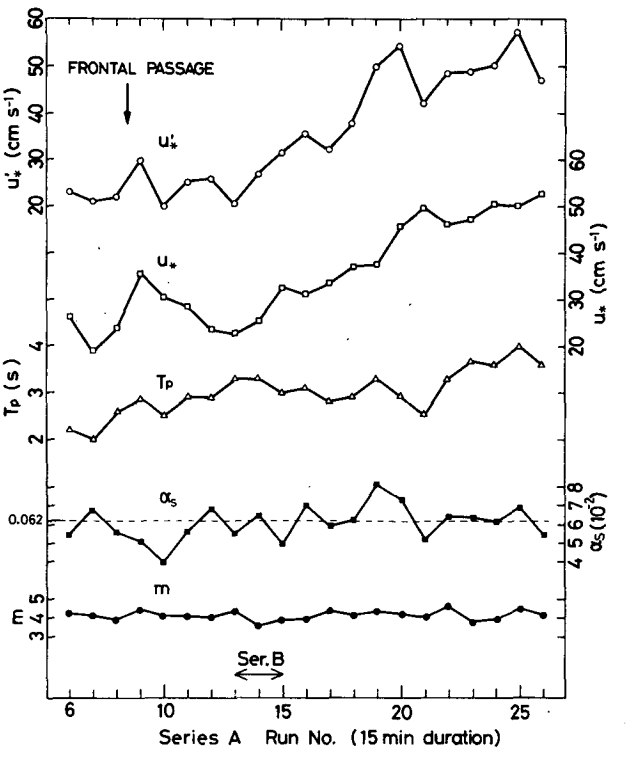

FIG. 1. Five-hour time series with data taken every fifteen minutes (Series A), obtained at the Shirahama Oceanographic Tower Station of Kyoto University. The data are reproduced from Tables 2 and 3 of Kawai et al. (1977).

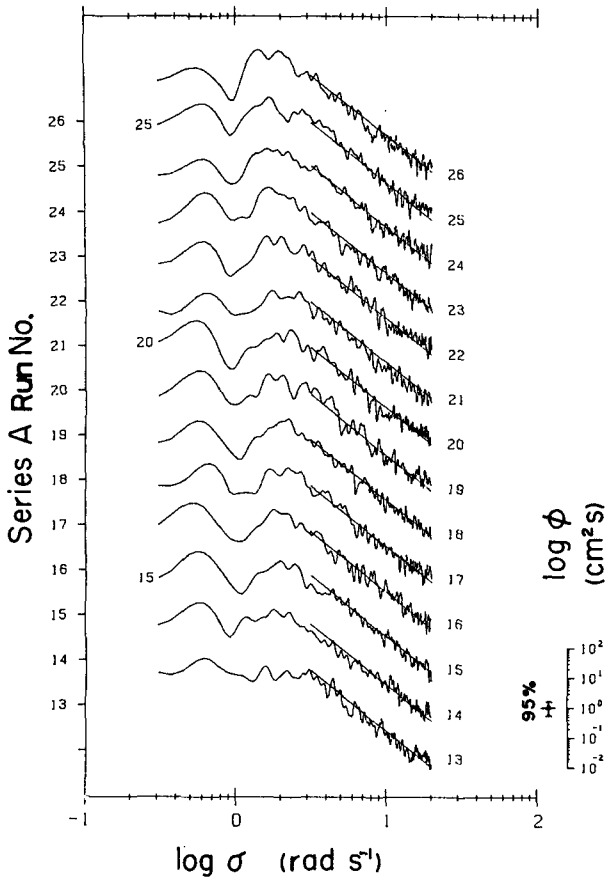

FIG. 2. The FFT wave spectra, recalculated using the original data used by Kawai et al. (1977) for runs 13 to 26.

Baylor wave gauge held tautly between two supports in the manner illustrated in Jones and Padman (1983).

The above sensors, together with some additional devices not relevant to this study, were coupled to an Evans-Hamilton Model 4046 Data Acquisition System. The data were digitized at 0.5 second intervals, and averages were recorded three times per hour on digital cassettes under microprocessor control.

The wave staff was calibrated approximately once a month by shorting the sensor at four depths (all above the sea surface) and comparing the observed reading with the measured position of the shorter bar. The data acquisition system can be put into a test mode in which the outputs from A/D converters are displayed on the front panel. The test mode was used for the calibrations discussed above and well-known voltages were also injected in place of the sensors, thus verifying the operation of the A/D converters.

3. Shirahama five-hour time series (Series A)

Using Tables 2 and 3 from Kawai et al. (1977), Fig. 1 shows the five-hour time series with 15-minute average values (Series A) of u_* and the wave period T_p corresponding to the spectral peak frequency, together with those of α, m and α_s, defined respectively by

$$\phi(\sigma) = \alpha\sigma^{-m}, \tag{4}$$

where m represents the best fit value of the observed spectra, and by

$$\phi(\sigma) = \alpha_s g u_* \sigma^{-4}; \tag{5}$$

u'_* is also defined as

$$u'_* = u_*(\alpha_s/\bar{\alpha}_s) \tag{6}$$

or

$$u'_* = \alpha/g\bar{\alpha}_s \quad \text{for} \quad m = 4, \tag{7}$$

where $\bar{\alpha}_s$ is the temporal average value of α_s. The friction velocity is u_*, which was determined from profiles

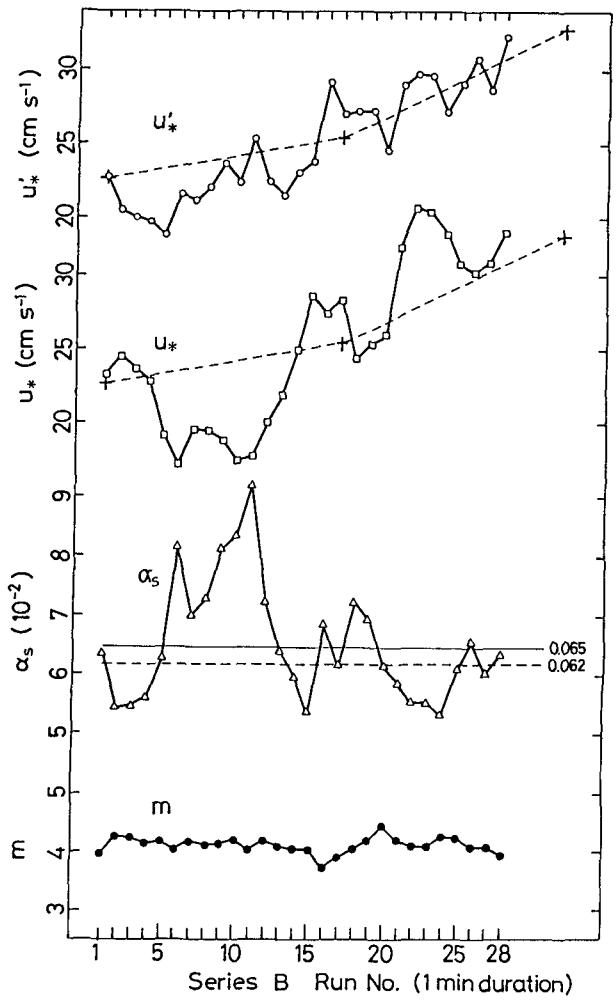

FIG. 3. Continuous data of 30-minute length (Series B) during runs 13 to 15 of Fig. 1, from Table 4 of Kawai et al. (1977). Crosses indicate 15-minute average values of u_* from Fig. 1.

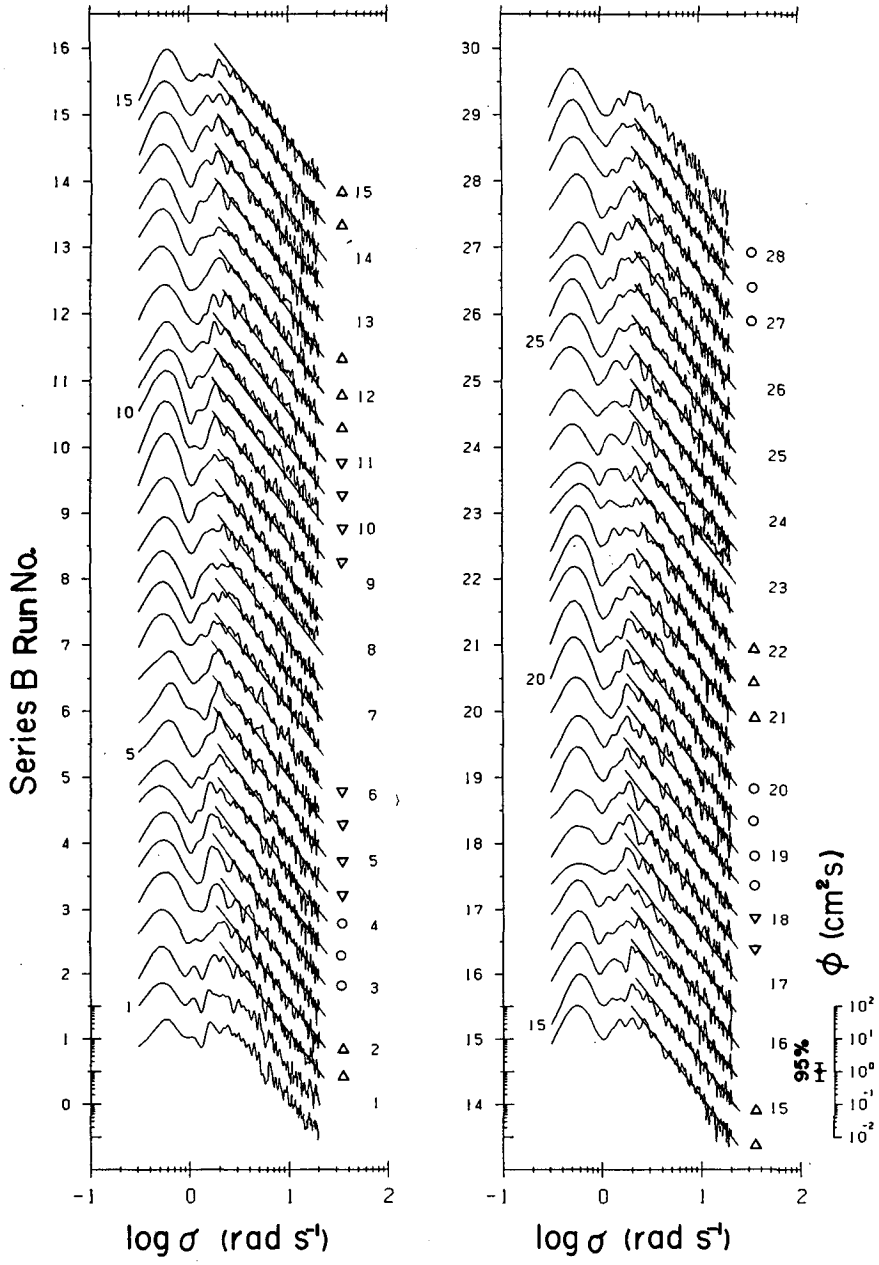

FIG. 4. Time series of FFT spectra of wind waves for Series B. Triangles, circles, and inverse triangles indicate typical cases of increasing, constant, and decreasing winds, respectively.

of the 15-minute averaged wind speed, while T_p was determined from the peak frequency of a spectra of 1.5 minutes of wave record in the middle of every 15 minutes. The α and m were determined from these spectra by using the method of least squares. (The range of frequencies used was indicated in Table 3.)

If the energy level of the equilibrium range of frequencies immediately follows the change of u_*, α_s would be a constant and u'_* would show the same variation as u_*. However, since the spectrum has an adjustment time scale, $T_{\alpha s}$, the coefficient α_s fluctuates with wind stress changes on time scales less than $T_{\alpha s}$, and hence u'_* differs from u_*. For changes in u_* slow compared with $T_{\alpha s}$, u'_* follows the trends of u_*. Thus, u'_* is presented to illustrate the variation of α, according to (7), anticipating that u'_* should have a trend similar to u_*. Up to run 8 in the Shirahama data, the swell was more important than after the passage of a front caused by the start of the winter monsoon. The wind had a fetch of several tens of kilometers.

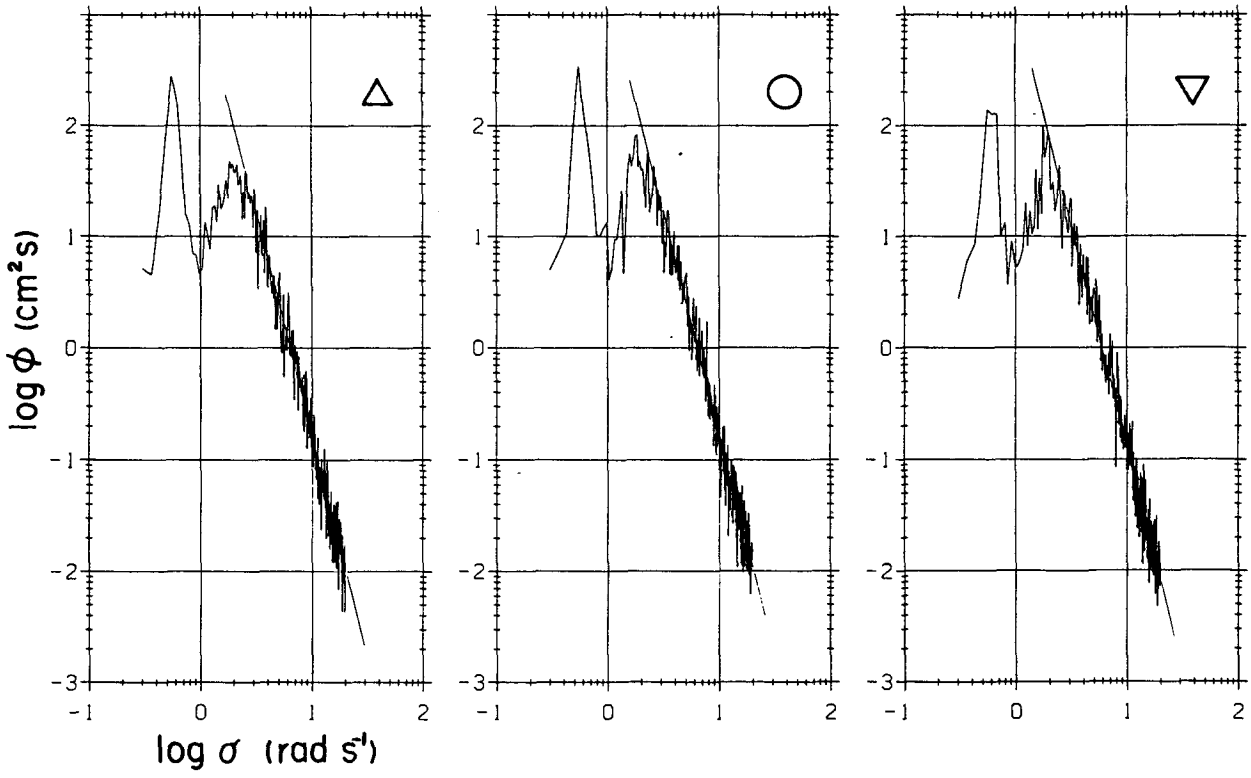

FIG. 5. Ensemble averages of ten of the raw spectra marked by triangles (increasing wind), circles (constant wind), and inverse triangles (decreasing wind), respectively, in Fig. 4.

It is seen in Fig. 1 that u'_* increases according to a trend similar to u_*, but m and α_s retain their nearly constant values throughout the fluctuations in wind speed. As already reported in Kawai et al. (1977) the average values and the standard deviations of m and α_s for this dataset are $m = 4.15 \pm 0.25$ and $\alpha_s = 0.062 \pm 0.010$, respectively. There is a tendency for α_s to be negatively correlated with the variation of u_* (on shorter time scales). This point will be discussed in the next section in more detail. It is also noted that a negative correlation of T_p with u_* is evident.

Figure 2 shows the FFT wave spectra, which have been recalculated using the original data for runs 13 to 26. The data used for each spectrum are 2048 data points sampled at 10 Hz, and a Hamming filter has been used five times. The inserted straight lines are drawn by using the appropriate u_* value with the mean value $\bar{\alpha}_s = 0.062$. It is seen that the peak frequency shifts with the change of wind and corresponds to the variation of T_p in Fig. 1. The increase in u_* causes the increase of α. If the total energy of the wind waves does not increase as rapidly, the upward shift of the high-frequency slope (increase of α) should be achieved at the expense of the energy of waves near peak frequency.

Furthermore, it seems that the increase in α also corresponds to a reduction in the swell energy, as seen, e.g., in runs 17, 21, 24 and 26, in Fig. 2. This may be a manifestation of nonlinear coupling.

4. Shirahama 30-minute continuous time series (Series B)

In Fig. 3 are shown, as Series B, continuous data of 30 minutes duration during runs 13 to 15 of Series A. This corresponds to Table 4 of Kawai et al. (1977). Fifteen-minute average values of u_* are shown by crosses. Again m maintains a value around 4 with a mean value of $m = 4.11 \pm 0.13$, and u'_* values follow the general trend of u_*, but the undulation of a time scale smaller than about ten minutes remains. The value of m is very close to 4 for increasing u_* but has a tendency to become slightly larger for decreasing u_*. The value of α_s shows a conspicuous variation having a negative correlation with the short time scale variation of the wind speed. The general trend of u_* in the 30-minute series is to increase, but the general trend of α_s is to remain constant, with an average value of $\alpha_s = 0.065 \pm 0.010$. This is interpreted as showing that the level of the high-frequency side of the spectra (the equilibrium range) adjusts itself to the trend (i.e., slow changes) of the wind, but cannot adjust itself to the variation of wind with time scales smaller than about 10 minutes.

Figure 4 shows a time series of spectra from Series B. This has been calculated from the original digitized time-series data used by Kawai et al. (1977), but FFT analysis has been applied to each 1024 data points from

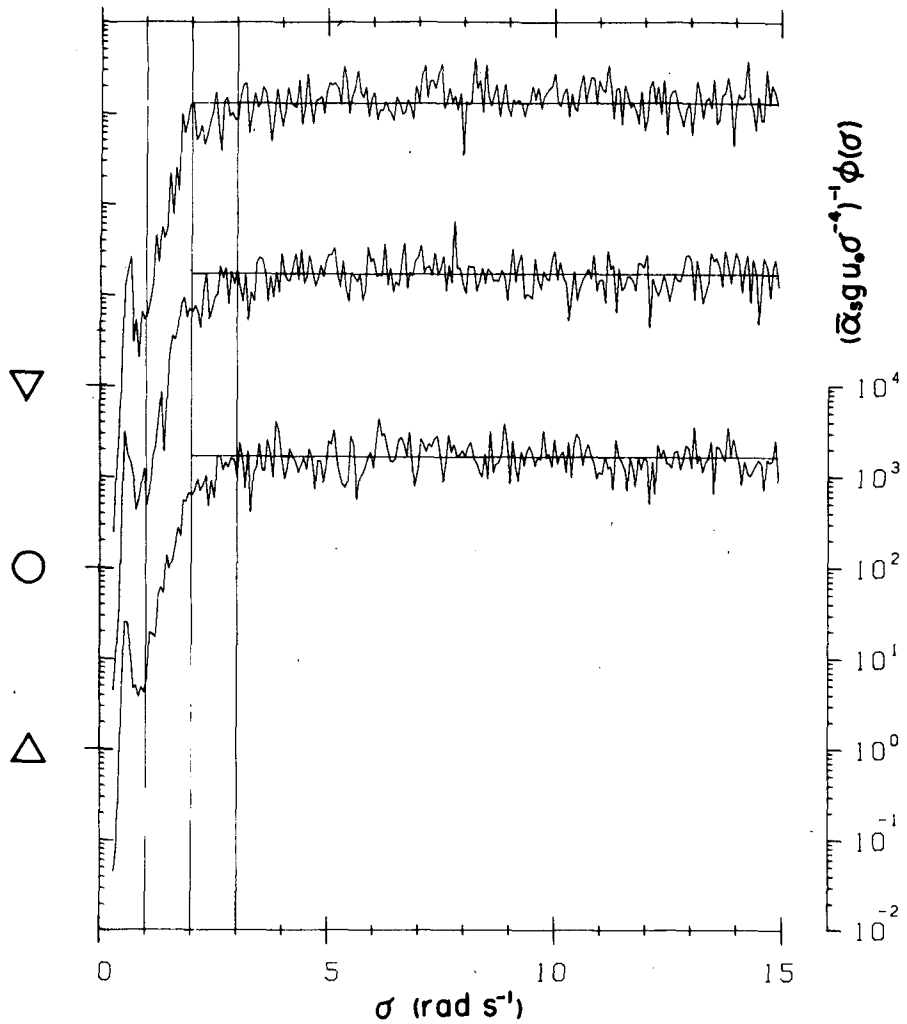

FIG. 6. As in Fig. 5, except normalized by the representative mean values of $\bar{\alpha}_s g u_* \sigma^{-4}$.

10 Hz sampling, moving through the time series in 30 s increments to produce about two-thirds overlap of data in each sequential spectra. Five passes of a Hamming filter have been applied. When u_* is increasing, the wind wave part of the spectra has a broad peak, as indicated by triangles; and when u_* is decreasing, it has a narrow peak, as indicated by inverse triangles.

Figure 5 shows the ensemble averages of ten of the raw spectra as marked by triangles, circles (constant wind), and inverse triangles. The aforementioned tendency of the peak can be clearly seen. In the case of increasing u_*, the peak is round on both sides; in the case of decreasing u_*, the peak is sharp on both sides, with a high peak value. The straight lines show (5) with the average value of α_s and u_* for the appropriate ten runs. Figure 6 shows the same spectra in a form normalized by the respective mean values of $\bar{\alpha}_s g u_* \sigma^{-4}$; the same tendency is clearly seen.

It appears that when u_* increases, the energy of the peak frequency wave quickly feeds energy to the waves on both sides of the spectral peak. When u_* decreases, the energy of the waves on the high frequency side of the peak (the equilibrium range) decreases and it is partly transferred into the waves around the peak; the energy of the waves on the low-frequency side is also transferred to the peak wave. This suggests that there is some effect that keeps the shape of the spectra around the peak rather symmetrical on a logarithmic diagram. The shape of the spectrum for the nonchanging winds lies between the increasing and the decreasing wind cases.

Since in Series B the time scale of the processes concerned is small, neither the total energy of the wind waves nor the peak frequency seem to change appreciably, in contrast to the longer term variation in the five-hour time series.

Based on the same transforms as Fig. 4, a time series of the spectra of Series B, normalized by $\alpha_s g u_* \sigma^{-4}$, is shown in Fig. 7. Each spectrum is generally independent of σ above a spectral peak of $\sigma_p \approx 2$ rad s^{-1}, but

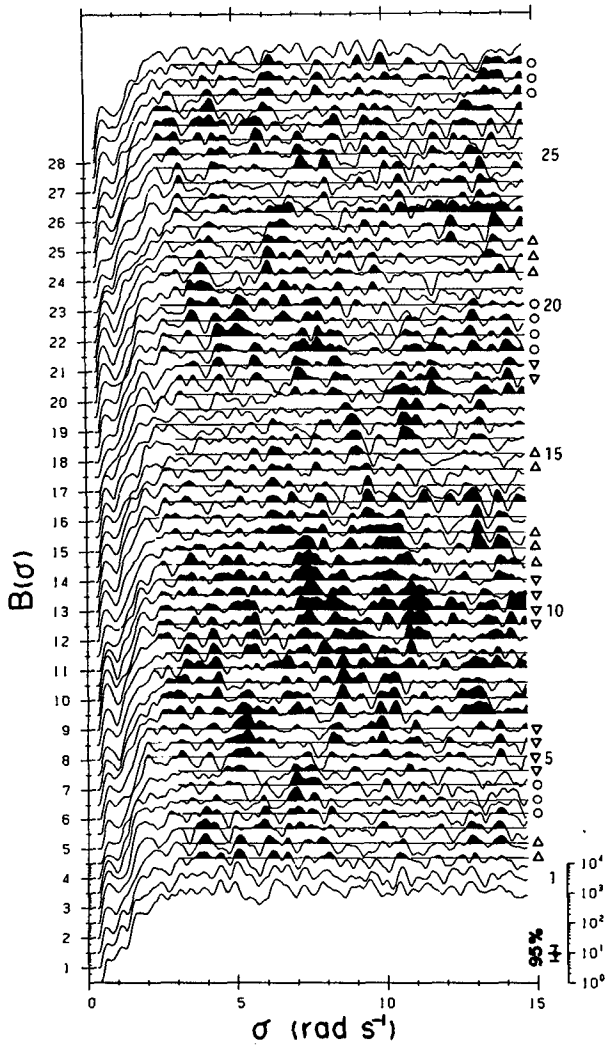

FIG. 7. As in Fig. 4, except normalized by $\bar{\alpha}_s g u_* \sigma^{-4}$. The shaded area represents values larger than unity of the degree of saturation defined by (8).

there are smaller scales of undulations of the order of 1 rad s^{-1} in the frequency scale. In order to trace the change in the spectra, the shaded area shows the part above the line of normalization. The quantity plotted is conceptually similar to Phillips's "degree of saturation" (1984), though the definition is different, namely,

$$B(\sigma) = (\bar{\alpha}_s g u_* \sigma^{-4})^{-1} \phi(\sigma). \quad (8)$$

Since the data length used is 102.4 seconds, or approximately 1.7 min for each spectrum, the adjacent spectra are made from partly overlapping data. However, spectra 2 minutes apart are completely independent of each other. One can trace some excesses or deficits in the degree of saturation for a considerable time if the frequency of excess saturation is considered to shift to larger or smaller values. Sometimes one region of excess bifurcates and a new deficit grows in between. Sometimes two regions of excess merge to become one. These features are partly a result of a kind of interpolation between the independent spectra. However, though single values of power spectral density vary within the 95% confidence limit, which is shown in the figure, the consistent characteristics of these variations in the degree of saturation encourage us to believe those observations are more than statistical fluctuation. The variation of the normalized spectra reminds us of resonant nonlinear wave interactions, but it should be noted that the actual energy level becomes small with increasing σ. The distribution of regions of excess saturation seems nearly uniform across the spectrum.

Figure 8 shows the time variation of the saturation spectra $B(\sigma, t_0)$, where t_0 is the run number. The frequency scale of the excesses or deficits in saturation is about 1 rad s^{-1} and the time scale is of the order of several minutes. To examine the patterns in the fluctuation in saturation spectra, the values of $B(\sigma, t_0)$ were transformed for frequencies $3.0 < \sigma < 14.9$. The resultant two-dimensional spectra is shown in Fig. 9 and has about 20 degrees of freedom due to a 2D Hamming filter. One axis is cycles per rad s^{-1}, while the other is cycles per minute. Two peaks are evident. Both have time scales of about $t^{-1} = 0.18$ min^{-1} (i.e., $t = 6$ min) but one is associated with fluctuations in frequency of 0.8 cycle per rad s^{-1}, while the other occurs at 0.3 cycle per rad s^{-1}. These peaks are the patterns in $B(\sigma, t_0)$ in Fig. 8 that seems to "propagate" in time across the frequency axis.

Young et al. (1987) have commented on how, in their numerical experiments, nonlinear processes redistribute spectral anomalies to stabilize the spectral shape. Figure 8 may reflect such a process of redistributing energy to neighboring frequency bands, though more strongly nonlinear processes such as wave breaking may also be included.

5. Bass Strait sixty-minute time series (Series C)

Waves of much greater amplitude than at Shirahama were observed in Bass Strait in 1978. Consequently the 256 heights used in the FFT were prewhitened to reduce the spectral distortion. The wind was in general rising for almost 24 hours before the measurements were made. It reached about 20 m s^{-1} and was somewhat constant for the first 40 minutes presented in Fig. 10. It then rose to about 22 m s^{-1} over the next 20 minutes, but the 15-minute averaged wind direction varied less than 2 degrees. For this second rising period the average value of α_s calculated for frequencies between 0.4 Hz and 0.8 Hz was $\alpha_s = 0.068$, a value very close to that observed at Shirahama. Though the general trend of α_s is nearly a constant, an inverse correlation with u_* is seen here also, for the variation of u_* of the time scale smaller than 20 minutes. During this one-hour period the currents were low, of the order of 0.03 m s^{-1}, while the significant wave height was between 5

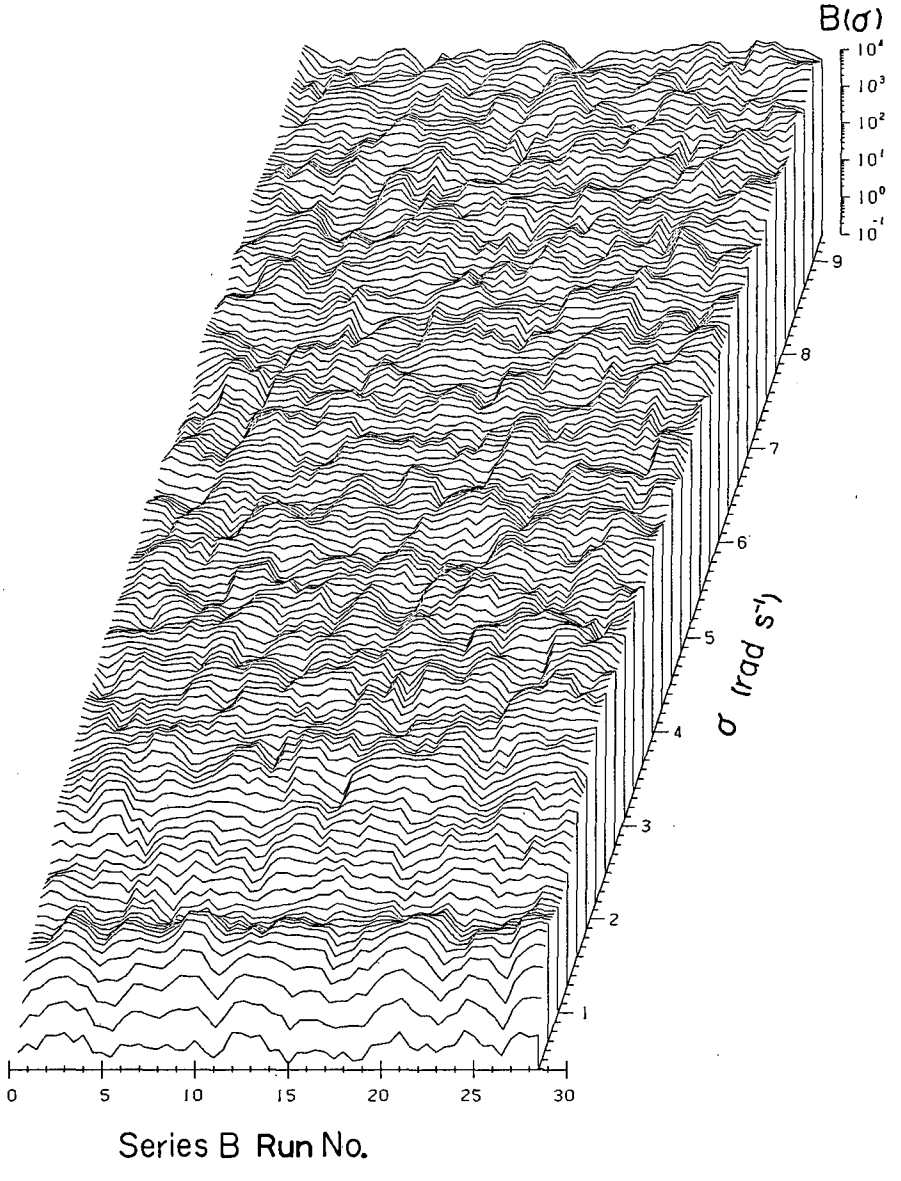

FIG. 8. Time variation of the "degree of saturation" shown in Fig. 7 for fixed frequencies.

and 6 m and the zero crossing period between 8 and 10 seconds.

6. Discussion

The similarity laws for the local equilibrium of wind waves describe a condition toward which waves evolve. The factor α_s for the "equilibrium range" of frequencies above the wave spectral peak is a "universal constant" only for slowly varying winds and varies in response to rapidly increasing or decreasing wind speeds (or presumably direction). Phillips (1985) pointed out that the empirical average values of α_s varied from the 0.062 of Kawai et al. (1977) and the 0.087 of Mitsuyasu et al. (1980) to the 0.11 of Kahma (1981) and Forristall (1981). Battjes et al. (1987) reported an average value of 0.13. There are some difficulties with the different methods of determining the friction velocity u_*. This is a subject that merits further study. The difference in α_s may also be due to the underlying current, which was not always reported, as Battjes et al. (1987) have suggested. Our two experiments showed good agreement both for the slowly rising trends and for the period of almost no trend at the start of Series C. Mitsuyasu et al. (1980) suggested that the α_s may be fetch dependent; but our two experiments at very different fetch do not support this suggestion. The role of peak enhancement or of swell in influencing the value of α_s deserves further investigation.

The value of m also has a weak variation: for rapidly increasing u_*, m becomes close to 4, and for rapidly decreasing u_*, it becomes slightly larger. A commonly reported tendency—that average values of m are slightly larger than 4—seems to come from this fact.

Accordingly, it is plausible that, for situations in which the wind changes rapidly, the energy input from the wind, spectral flux divergence by nonlinear wave interactions, and loss by breaking are not proportional to one another as Phillips (1985) assumed for the equilibrium range. In the case of increasing u_*, the input and dissipation may increase before the nonlinear interaction term, while in the case of decreasing u_*, the spectral flux divergence may become the dominant term and transfer energy in the frequency direction opposite to that of equilibrium.

When the wind increases rapidly, the degree of saturation becomes smaller than unity since the spectral level takes time to reflect the increase in u_*. With a larger u_* the supply of energy to the equilibrium range waves by the wave–wave interactions increases at the expense of the energy of waves near the spectral peak. Physically, the form of the individual waves becomes distorted, leaning forward (Bailey et al. 1988, have shown that the wave shape can be expressed as a function of C/u_*), and wave breaking of the waves near the peak frequency feeds energy to waves on both sides. For a while, the peak frequency shifts toward the high-frequency side, until the energy input from the wind restores the deficit of the energy needed for a new equilibrium.

When the wind decreases rapidly, the energy loss by wave breaking may decrease, and the form of the individual waves may become less distorted. Slowly the energy level of the equilibrium range of frequencies reduces to its lower new equilibrium value. In view of the form of the spectral adjustment, we suspect that the wave interactions transfer excess energy from higher to lower frequencies, which is in the direction opposite to that in the rising wind case. This increases the energy of the peak wave, and for a while the peak frequency shifts to a lower value.

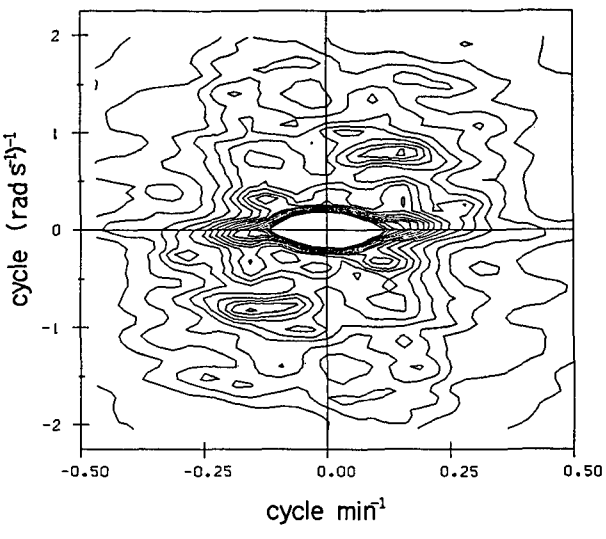

FIG. 9. Two-dimensional spectrum of the values $B(\sigma, t_0)$ of Fig. 8, in the range of frequencies $3.0 < \sigma < 14.9$.

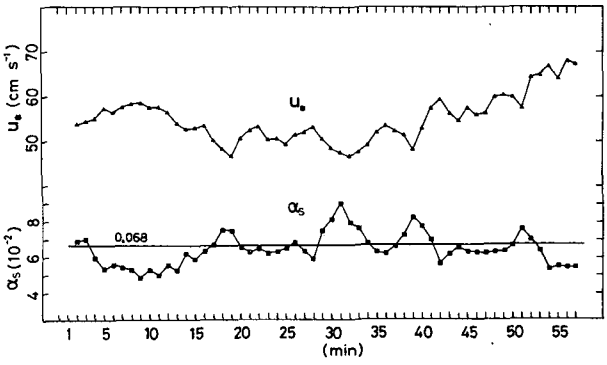

FIG. 10. Sixty-minute time series of u_* and α_s in Bass Strait, Series C. Three-minute average values are plotted.

From the above data, the time scale of these processes seems to be less than several minutes to change α_s and 10 to 15 minutes to produce a shift in the peak frequency.

The tendency of the spectral shapes to have a symmetrical appearance in the logarithmic representation (around the peak frequency) was already noted in the context of Fig. 5. If we assume a symmetrical spectral form, the complete spectra is expressed by

$$\phi(\sigma) = \alpha_s g u_* \sigma^{-4} \qquad (\sigma \geq \sigma_p)$$

$$\phi(\sigma) = \alpha_s g u_* \sigma_p^{-8} \sigma^4 \quad (\sigma \leq \sigma_p). \tag{9}$$

This form, taken from the TOHOKU Wave Model (Joseph et al. 1981; Toba et al. 1985a; Toba et al. 1985b), allows intergration to produce

$$E = \int_0^\infty \phi(\sigma) d\sigma. \tag{10}$$

An alternative form of (2) was presented in Toba (1978) as

$$E^* = B_\sigma \sigma_p^{*-3}, \tag{11}$$

where $B = 0.051$, $E^* = g^2 E / u_*^4$ and $\sigma_p^* = \sigma_p u_* / g$. Integration of the symmetrical spectral form, (9), when compared with (11), was shown by Joseph et al. (1981) to be

$$B_\sigma = \frac{8}{15} \alpha_s. \tag{12}$$

However, in the case in which there is peak enhancement, the right-hand side of (12) will be larger by some amount, say γ. Thus,

$$\alpha_s = \frac{15}{8}\frac{\beta_\sigma}{\gamma} = 0.096/\gamma. \qquad (13)$$

For the Shirahama data γ is near unity but for the Bass Strait data it was greater than unity. Thus the value of α_s between 0.06 and 0.07 in this study is only a little below that expected from (11).

Toba (1988) has proposed a physical concept of "wind-wave breaking adjustment" to provide a rationale for the similarity laws of wind waves, including (2) and (3). At the air–sea boundary, which includes the wind waves, in order to fulfill the overall constraints for the coupling of the two-sided turbulent boundary layer (i.e., air and water), proportionalities hold among the Stokes drift, the average surface velocity of water, the effective wind drift, the square root of the turbulent intensities above and below wind waves, and the friction velocities of air and water. It follows from the above model that the time scale of variation of α_s, due to changing winds represents the time scale of the processes of adjustment in the turbulent boundary layers above and below wind waves, and in turn, the time scale of above velocities.

Further detailed studies, using data on different scales of waves and changing winds, will be necessary to make these points more certain.

Acknowledgments. The authors express their thanks to Dr. K. Hanawa and Mr. N. Iwasaka for their kind help in the computation and presentation of data, together with much discussion. We wish to thank ESSO-BHP for allowing us to make measurements over a number of years from their Bass Strait platforms. This study has been partially supported by a Grant-in-Aid for Scientific Research from the Ministry of Education, Science and Culture, Number 61540294.

REFERENCES

Bailey, R. J., I. S. F. Jones and Y. Toba, 1988: The steepness and shape of wind waves. Manuscript to be published.

Battjes, J. A., T. J. Zitman and L. H. Holthuijsen, 1987: A reanalysis of the spectra observed in JONSWAP. *J. Phys. Oceanogr.*, **17**, 1288–1295.

Donelan, M. A., J. Hamilton and W. H. Hui, 1985: Directional spectra of wind-generated waves. *Phil. Trans. Roy. Soc. London*, **A315**, 509–562.

Forristall, G. Z., 1981: Measurements of a saturated range in ocean wave spectra. *J. Geophys. Res.*, **86**, 8075–8084.

Jones, I. S. F., and L. Padman, 1983: Semi-diurnal internal tides in Eastern Bass Strait. *Aust. J. Mar. Freshwater Res.*, **34**, 159.

Joseph, P. S., S. Kawai and Y. Toba, 1981: Ocean wave prediction by a hybrid model—Combination of single-parameterized wind waves with spectrally treated swells. *Tohoku Geophys. J.* (Sci. Rep. Tohoku Univ., Ser. 5), **28**, 27–45.

Kahma, K. K., 1981: A study of the growth of the wave spectrum with fetch. *J. Phys. Oceanogr.*, **11**, 1503–1515.

Kawai, S., K. Okada and Y. Toba, 1977: Support of the three-seconds power law and the $gu_*\sigma^{-4}$-spectral form for growing wind waves with field observational data. *J. Oceanogr. Soc. Japan*, **33**, 137–150.

Kitaigorodskii, S. A., 1983: On the theory of the equilibrium range in the spectrum of wind-generated gravity waves. *J. Phys. Oceanogr.*, **13**, 816–827.

Mitsuyasu, H., F. Tasai, T. Suhara, S. Mizuno, M. Ohkusu, T. Honda and K. Rikiishi, 1980: Observation of the power spectrum of ocean waves using a cloverleaf buoy. *J. Phys. Oceanogr.*, **10**, 286–296.

Phillips, O. M, 1958: The equilibrium range in the spectrum of wind-generated waves. *J. Fluid Mech.*, **4**, 426–434.

——, 1984: On the response of the short ocean wave components at a fixed wavenumber to ocean current variations. *J. Phys. Oceanogr.*, **14**, 1425–1433.

——, 1985: Spectral and statistical properties of the equilibrium range in wind-generated gravity waves. *J. Fluid Mech.*, **156**, 505–531.

Toba, Y., 1972: Local balance in the air–sea boundary processes, I. On the growth process of wind waves. *J. Oceanogr. Soc. Japan*, **28**, 109–120.

——, 1973: Local balance in the air–sea boundary processes, III. On the spectrum of wind waves. *J. Oceanogr. Soc. Japan*, **29**, 209–220.

——, 1978: Stochastic form of the growth of wind waves in a single-parameter representation with physical implications. *J. Phys. Oceanogr.*, **8**, 494–507.

——, 1987: Similarity laws of the wind wave and the coupling process of the air and water turbulent boundary layers. *Fluid Dyn. Res.* **2**, 000–000.

——, S. Kawai and P. S. Joseph, 1985a: The Tohoku wave model. *Ocean Wave Modeling*, The SWAMP Group, 201–210.

——, ——, K. Okada and N. Iida, 1985b: The Tohoku-II wave model. *The Ocean Surface*. Y. Toba and H. Mitsuyasu, Eds. D. Reidel, 227–232.

——, H. Kunishi, K. Nishi, S. Kawai, Y. Shimada and N. Shibata, 1971: Study of the air-sea boundary processes at the Shirahama Ocenaographic Tower Station. Disaster Prevention Res. Inst., Kyoto University, *Annals*, **14B**, 519–531 (in Japanese with English abstract).

Wu, J., 1980: Wind-stress coefficients over sea surface near neutral conditions—A revisit. *J. Phys. Oceanogr.*, **10**, 727–740.

Young, I. R., S. Hasselmann and K. Hasselmann, 1987: Computations of the response of a wave spectrum to a sudden change in wind direction. *J. Phys. Oceanogr.*, **17**, 1317–1338.